

Copper Silicide/Silicon Nanowire Heterostructures: *In-Situ* TEM Observation of Growth Behaviors and Electron Transport Properties

Chung-Hua Chiu^a, Chun-Wei Huang^a, Jui-Yuan Chen^a, Yu-Ting Huang^a, Jung-Chih Hu^b, Lien-Tai Chen^b, Cheng-Lun Hsin^c, and Wen-Wei Wu^{a*}.

^a Department of Materials Science and Engineering, National Chiao Tung University, Hsinchu 300, Taiwan

^b Nanotechnology Research Center, Industrial Technology Institute (ITRI), Chutung, Hsinchu, Taiwan 31040, R.O.C

^c Department of Electrical and Engineering, National Central University, Tao Yuan 320, Taiwan

*Address Correspondence to wwwu@mail.nctu.edu.tw

Table of Contents:

Fig. S-1: The fabrication procedures of *in-situ* TEM samples.

Fig. S-2: The effect of the temperature on the growth of copper silicides, from 350 to 600 °C.

Fig. S-3: HRTEM images of η -Cu₃Si of different zone axes: (a) [-12-13]; (b) [2-1-16].

Fig. S-4: Schematic diagrams of different nucleation type. (a) half-circular and (b) circular disk on the η -Cu₃Si/Si interface.

Supporting video-1: The observation of low magnification *in situ* TEM video of Cu₃Si grown at 450 °C.

Supporting video-2: The observation of low magnification *in situ* TEM video of Cu₃Si grown at 350 °C.

Supporting video-3: The observation of high resolution *in situ* TEM video of Cu₃Si grown at 350 °C.

To investigate the mechanism of copper silicide formation and electrical transport properties, Si NWs were firstly detached in ethanol solution by ultrasonic vibration and then dispersed on the membrane samples. The $\text{SiO}_2/\text{Si}_3\text{N}_4$ layers, with thickness of 30/60nm, were grown by low pressure chemical vapor deposition (LPCVD). Copper pads were carried out by e-beam lithography, metal deposition and lift-off processes, as shown in Fig. S-1.

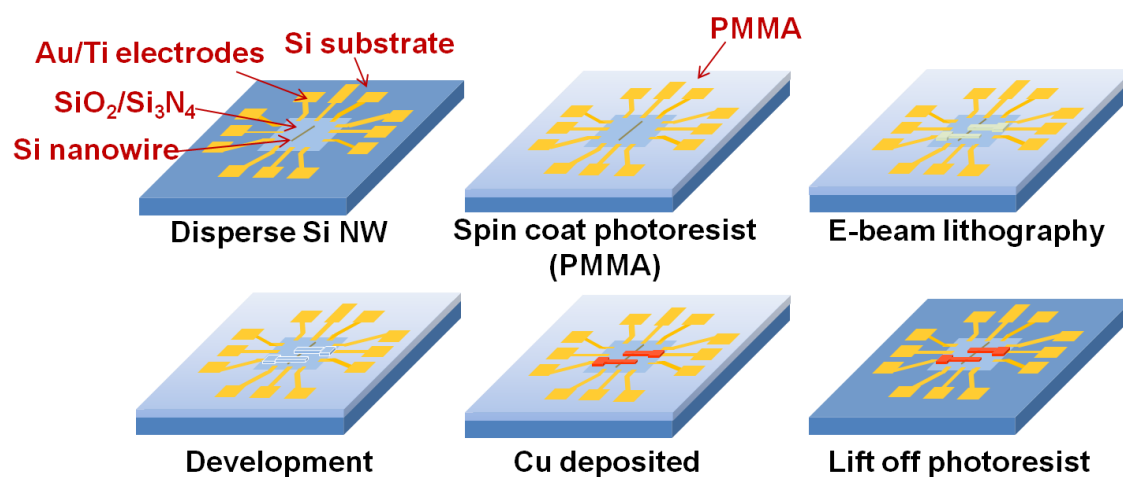


Fig. S-1 The fabrication procedures of *in-situ* TEM samples.

To investigate the effect of the temperature on the growth of copper silicides, various temperatures (from 350 to 600 °C) have been performed. Figures S-2 (a)-(c) are the HRTEM images of the copper silicide, showing the phases of $\text{Cu}_{15}\text{Si}_4$, η'' - Cu_3Si , and η - Cu_3Si , respectively, and the insets are the corresponding FFT diffraction patterns. Thus, phase/structure and kinetics analysis of the copper silicide grown at different temperatures was discussed.

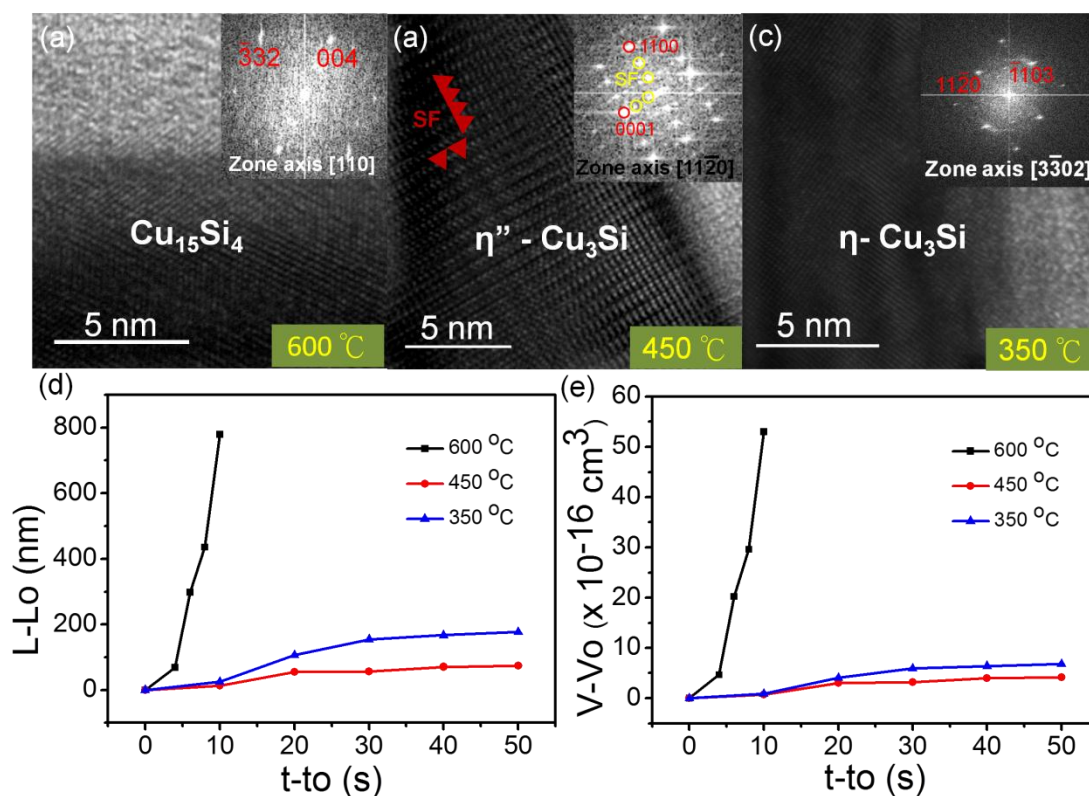


Fig. S-2 (a)-(c) HRTEM images of different phases through various reaction temperatures. The insets show the corresponding FFT diffraction patterns. (d) Plot of length vs. reaction time at different temperatures, illustrating a roughly linear growth rate at 600 °C. (e) Plot of the copper silicide volume vs. reaction time at various temperatures.

To further confirm the copper silicide structure grown at 350 °C we have analyzed the η -Cu₃Si structure from higher symmetry zone axes, and the insets are the corresponding FFT diffraction patterns.

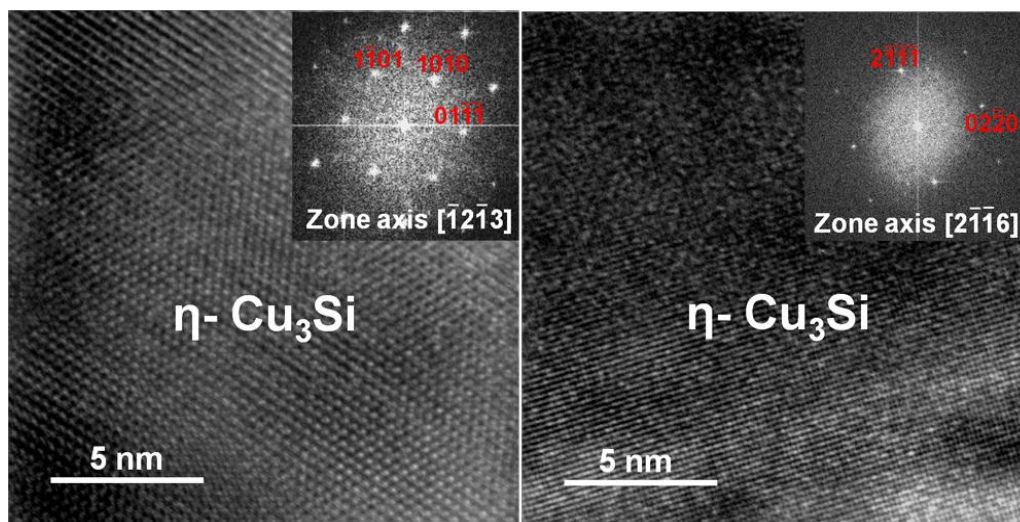


Fig. S-3: HRTEM images of η -Cu₃Si phase with different zone axes: (a) $[-12\bar{1}3]$; (b) $[2\bar{1}16]$.

Derive activation energy of heterogeneous and homogeneous nucleation.

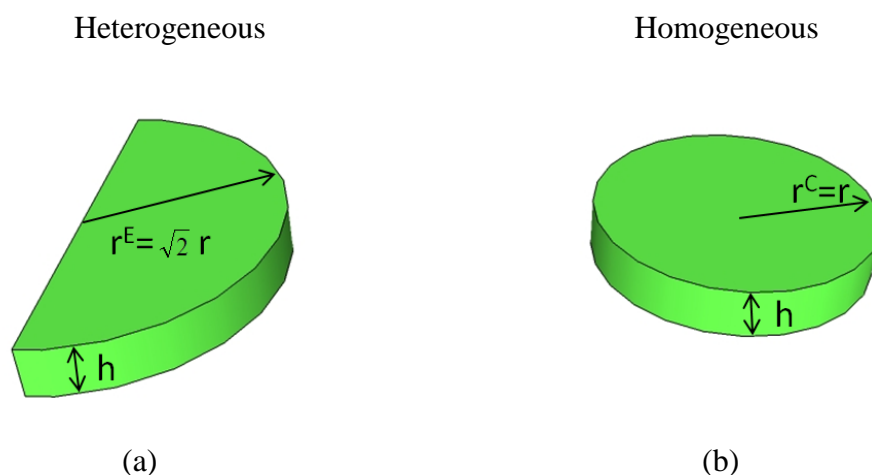


Fig. S-4 Schematic diagrams of different nucleation type. (a) half-circular and (b) circular disk on the η -Cu₃Si/Si interface.

The nucleation type we discussed at η -Cu₃Si/Si interface focused on a newly/initially nucleated η -Cu₃Si atomic layer. Therefore, the diameter of η -Cu₃Si nanowire close to the η -Cu₃Si/Si interface will be similar to that of the original Si nanowire as shown in Fig.2 (d) and (e). The similar V_{disc} but different shape in the two cases at center and edge are denoted as C and E. We consider the similar atomic height h with critical nuclei radius r and $\sqrt{2}r$ of homogeneous and heterogeneous nucleation, respectively. This is reasonable to assume the nucleation of a circular disk at center and a half-circular disk with similar height at edge sites^{41,42}

In homogeneous nucleation of a circular disk, the net change of free energy is

$$\Delta G^C = (V_{disc}^C \Delta g_v + A_{silicide/Si}^C \gamma_{silicide/Si}^C)$$

$$= -\pi r^2 h \Delta g_v + 2\pi r h \gamma_{silicide/Si}^C$$

Where V_{disc} is the critical volume of nuclei when the nucleation occurred, Δg_v is the change in free energy of formation of the silicide per unit volume, A is the additional interface area, and γ is the interfacial energy per unit area, respectively. The upper and lower cases in these notations denote the different nucleation site and interface, respectively.

The critical size of nuclei and activation energy are obtained through the first order differentiation of the above equation.

$$\frac{\partial \Delta G^C}{\partial r} = -2\pi r h \Delta g_v + 2\pi h \gamma_{silicide/Si}^C = 0$$

$$\Rightarrow 2\pi r h \Delta g_v = 2\pi h \gamma_{silicide/Si}^C$$

$$\Rightarrow r^{*C} = \frac{\gamma_{silicide/Si}^C}{\Delta g_v}$$

$$\Delta G^{*C} = \frac{\pi h \gamma_{silicide/Si}^{2C}}{\Delta g_v}$$

In heterogeneous nucleation of a half-circular disk, the net change of free energy is

$$\begin{aligned} \Delta G^E &= (V_{disc} \Delta g_v + A_{silicide/Si}^E \gamma_{silicide/Si}^E + A_{silicide/oxide}^E \gamma_{silicide/oxide}^E - A_{Si/oxide}^E \gamma_{Si/oxide}^E) \\ &= -\pi r^2 h \Delta g_v + \sqrt{2} \pi r h \gamma_{silicide/Si}^E + 2\sqrt{2} r h \gamma_{silicide/oxide}^E - 2\sqrt{2} r h \gamma_{Si/oxide}^E \end{aligned}$$

The critical size of nuclei and activation energy are obtained through the first order differentiation of the above equation.

$$\frac{\partial \Delta G^E}{\partial r} = -2\pi r h \Delta g_v + \sqrt{2} \pi h \gamma_{silicide/Si}^E + 2\sqrt{2} h \gamma_{silicide/oxide}^E - 2\sqrt{2} h \gamma_{Si/oxide}^E = 0$$

$$\Rightarrow 2\pi r h \Delta g_v = \sqrt{2} h (\pi \gamma_{silicide/Si}^E + 2\gamma_{silicide/oxide}^E - 2\gamma_{Si/oxide}^E)$$

$$\Rightarrow r^{*E} = \frac{\sqrt{2} (\pi \gamma_{silicide/Si}^E + 2\gamma_{silicide/oxide}^E - 2\gamma_{Si/oxide}^E)}{2\pi \Delta g_v}$$

We note that $\gamma_{silicide/oxide}^E \gg \gamma_{Si/oxide}^E$

$$\Rightarrow r^{*E} \approx \frac{\sqrt{2} (\pi \gamma_{silicide/Si}^E + 2\gamma_{silicide/oxide}^E)}{2\pi \Delta g_v}$$

$$\Delta G^{*E} \approx -\pi h \Delta g_v \frac{2(\pi^2 \gamma_{silicide/Si}^{2E} + 4\pi \gamma_{silicide/Si}^E \gamma_{silicide/oxide}^E + 4\gamma_{silicide/oxide}^{2E})}{4\pi^2 \Delta g_v^2} +$$

$$\frac{2\pi h (\pi \gamma_{silicide/Si}^{2E} + 2\gamma_{silicide/oxide}^E \gamma_{silicide/Si}^E)}{2\pi \Delta g_v} + \frac{4h (\pi \gamma_{silicide/Si}^E \gamma_{silicide/oxide}^E + 2\gamma_{silicide/oxide}^{2E})}{2\pi \Delta g_v}$$

$$= \frac{\pi h \gamma_{silicide/Si}^{2E}}{2\Delta g_v} + \frac{2h \gamma_{silicide/Si}^E \gamma_{silicide/oxide}^E}{\Delta g_v} + \frac{2h \gamma_{silicide/oxide}^{2E}}{\pi \Delta g_v}$$

From the experimental results as shown in Fig. 4(a) and Video-3, every new η -Cu₃Si atomic layer always start from center of the Si NW. It indicated that the homogeneous nucleation dominates the η -Cu₃Si growth. Furthermore, the homogeneous nucleation of silicide growth has been demonstrated in our previous studies.^{41,42} Therefore, we consider that $\Delta G^{*E} \geq \Delta G^{*C}$ inequality will be satisfied.

$$\Rightarrow \frac{\pi h \gamma_{\text{silicide/Si}}^E}{2\Delta g_v} + \frac{2h \gamma_{\text{silicide/Si}}^E \gamma_{\text{silicide/oxide}}^E}{\Delta g_v} + \frac{2h \gamma_{\text{silicide/oxide}}^E}{\pi \Delta g_v} \geq \frac{\pi h \gamma_{\text{silicide/Si}}^C}{\Delta g_v}$$

$$\Rightarrow \frac{2h \gamma_{\text{silicide/Si}}^E \gamma_{\text{silicide/oxide}}^E}{\Delta g_v} + \frac{2h \gamma_{\text{silicide/oxide}}^E}{\pi \Delta g_v} \geq \frac{\pi h \gamma_{\text{silicide/Si}}^C}{2\Delta g_v}$$

$\gamma_{\text{silicide/Si}}$ is considered the same regardless of the different nucleation sites. Hence, we

note that $\gamma_{\text{silicide/Si}}^E = \gamma_{\text{silicide/Si}}^C = \gamma_{\text{silicide/Si}}$ equality is satisfied.

$$\Rightarrow \left(\frac{2}{\pi} \gamma_{\text{silicide/oxide}}^E + 2\gamma_{\text{silicide/Si}} \gamma_{\text{silicide/oxide}}^E - \frac{\pi}{2} \gamma_{\text{silicide/Si}}^2 \right) \geq 0$$

$$\Rightarrow \frac{2}{\pi} (\gamma_{\text{silicide/oxide}}^E + \frac{\pi}{2} \gamma_{\text{silicide/Si}})^2 \geq \pi \gamma_{\text{silicide/Si}}^2$$

$$\Rightarrow \gamma_{\text{silicide/oxide}}^E \geq \left(\frac{\pi}{\sqrt{2}} - \frac{\pi}{2} \right) \gamma_{\text{silicide/Si}}$$

$$\Rightarrow \gamma_{\text{silicide/oxide}}^E \geq 0.65 \gamma_{\text{silicide/Si}}$$

In-situ TEM videos of the dynamic reaction of the copper silicide/Si/copper silicide nanowire heterostructures.

Supporting video-1: The video shows the dynamic growth process of Cu_3Si . At 450 °C, the formation of stacking faults may decrease the reaction rate since higher activation energy would be necessary to nucleate Cu_3Si .

Supporting video-2: The video shows the dynamic growth process of Cu_3Si . At 350 °C, and it shows faster growth rate compared with that at 450 °C.

Supporting video-3: The video shows that the curvature presented near the edge of Si/oxide interface during the growth process. It may due to the high surface energy of silicide/oxide interface. Thus, it would hinder the formation of silicide.